Enhancement of Flame Blowout Limits by the Use of Swirl

DOUGLAS FEIKEMA, RUEY-HUNG CHEN, and JAMES F. DRISCOLL

Department of Aerospace Engineering, The University of Michigan, Ann Arbor, MI 48109-2140

The blowout limits of a number of swirl-stabilized, nonpremixed flames were measured, and the observed trends are successfully explained by applying certain concepts that previously have been applied only to nonswirling flames. It is shown that swirl flame blowout limits can be compared to well-known limits for nonswirling simple diffusion flames by using the proper nondimensional parameter, i.e., the inverse Damkohler number $(U_F/d_F)/(S_L{}^2/\alpha_F)$. The fuel velocity at blowout (U_F) was measured while four parameters were systematically varied: the fuel tube diameter (d_F), the fuel type and thus reaction rate, which is related to the maximum laminar burning velocity (S_L), the coaxial air velocity (U_A), and the swirl number. Results show that for zero swirl, the blowout curves agree with curves predicted by previous analysis. However, as swirl is added, the flame becomes five times more stable (based on maximum fuel velocity). To explain the effect of swirl, a simple analysis is presented that is an extension of previous nonswirling flame blowout theory. It shows that the conventional swirl number is not the appropriate governing parameter. Instead, a Damkohler number based on swirl velocity is suggested by the analysis and is found to help collapse the data at the rich blowout limit to a single, general curve. Swirl causes a jet-vortex interaction; the recirculation vortex reduces the fuel jet velocity on centerline, which strongly stabilizes the lifted flame. As one increases the fuel tube diameter or the reaction rate (by adding hydrogen), the swirl flame becomes more stable, in a manner similar to a nonswirling flame. Another advantage of swirl is that it makes overall fuel-lean operation possible; the present flame is unstable without swirl for fuel-lean conditions.

NOMENCLATURE

d_A	air tube inner diameter (Fig. 1)
d_F, $d_{F,0}$	fuel tube inner, outer diameter
$\mathrm{Da}_K{}^{-1}$	critical inverse Damkohler number for jet flame blowout, given by Kalghatgi (Eq. 3)
$\mathrm{Da}_B{}^{-1}$	critical inverse Damkohler number for jet flame blowout, given by Broadwell et al. (Eq. 5)
$\mathrm{Da}_0{}^{-1}$	critical inverse Damkohler number measured for $U_A = 0$
S	swirl number at throat
S_g	geometric swirl number at throat, as given by Eq. 7
S_L, S_T	maximum laminar, turbulent burning velocity
U_A	axial air velocity at throat location defined in Fig. 1
U_{CL}	axial velocity on centerline
U_F	axial fuel velocity at fuel tube exit
U_j	axial velocity on centerline induced by fuel jet only
U_{RZ}	characteristic recirculation zone velocity
U_v	axial velocity on centerline induced by recirculation vortex
U_θ	characteristic angular velocity at throat, equal to $U_A \cdot S$
$U_{\theta,c}$	critical angular velocity at throat required for onset of recirculation
α_F, ν_F	thermal diffusivity, kinematic viscosity of the fuel
α_S	thermal diffusivity of stoichiometric, hot gas in flame (=4.56 cm^2/s in BDM analysis)
δ	fuel jet halfwidth
ϕ_0	overall fuel-air equivalence ratio, based on inlet mass flows

Published by Elsevier Science Publishing Co., Inc.
655 Avenue of the Americas, New York, NY 10010

0010-2180/90/$3.50

INTRODUCTION

The purpose of this article is to report some systematic measurements of the blowout limits of swirl-stabilized flames and to explain the measured trends using concepts that have been successfully used in nonswirling flames. The swirl flame that was studied can be described, in simplest terms, to be a fuel jet that passes through the center of a strong toroidal vortex. The vortex is the recirculation zone that is created when swirl is added to a coaxial airstream that surrounds the fuel jet (Fig. 1). Properties of the present flame [1–4] and other swirl flames [5, 6] have been well documented because swirl is commonly used in gas turbine engines, industrial burners, and advanced ramjet designs [7] and dump combustors [8]. The resulting jet–vortex interaction is known to stabilize the flame, but the reasons for the stabilizing effects are still in dispute. Some of the major questions that the present work addresses are as follows:

1. Which of several proposed mechanisms correctly explains how the flame–vortex interaction (which is cased by the swirl) increases the stability of a flame?
2. How do blowout limits of swirl flames scale as the burner size is increased and the fuel type is varied?
3. What parameter should one use to compare blowout limits of swirl flames to the limits for a simple jet flame in order to see if swirl is indeed beneficial?

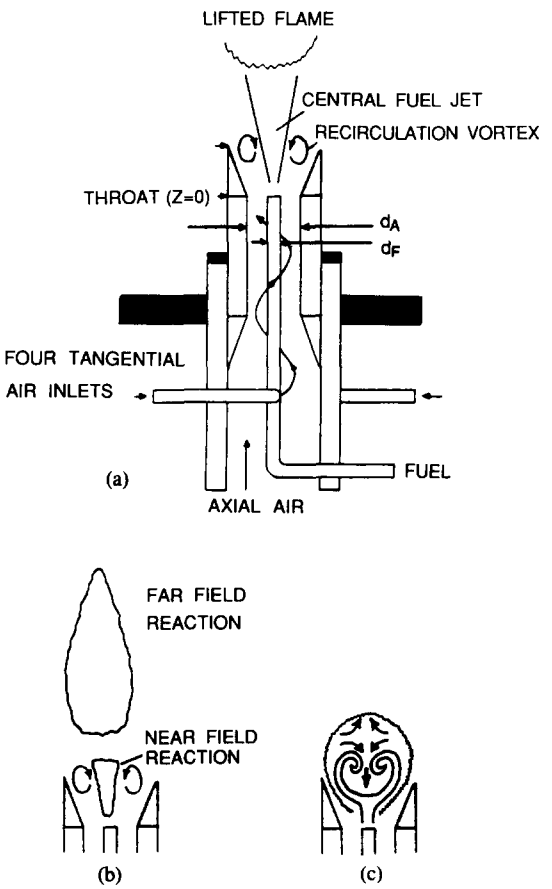

Fig. 1. Schematic of Flame Appearance at Blowout. (a) Lifted flame at rich limit. (b) Split, jet-like flame (type 1) at rich limit. (c) Short, strongly recirculating flame (type 2) at lean limit (no liftoff).

Some reasons why swirl enhances flame stability have been offered by Leuckel and Fricker [9], Rawe and Kremer [10], and Yuasa [11]. In addition, the blowout limits of some swirl flames (for a limited range of conditions) also have been reported by Tangirala et al. [1], Whitelaw [12], and others [13, 14]. It is clear from the above work that there are three ways in which flame blowout occurs, which can be labeled: (1) the excessive fuel velocity limit (or the "rich limit"), (2) the excessive swirl and/or air velocity limit (or the "lean limit"), and (3) the minimum swirl limit, which leads to the disappearance of the recirculation vortex.

The effect of swirl on flame blowout still is in dispute. At present, there are four different mechanisms that attempt to explain the effect of swirl:

1. Swirl is believed to be a stabilizing factor because it increases the turbulent *burning velocity* of the base of a lifted flame [9, 10, 14]. The base region of a lifted, initially nonpremixed flame most likely is partially premixed. Swirl should increase the turbulent burning velocity at the flame base because it increases the local velocity fluctuations by a factor of three [1] and because the recirculation vortex should create larger regions of locally premixed fuel and air than are found in nonswirling flames.

2. A different proposal is that the recirculation vortex acts as a *heat source*, forcing hot products to move upstream and mix with the partially premixed reactants [5]. Thus swirl can increase the residence time during which fuel, air, and hot products can coexist, which could be an important stabilizing factor near the blowout limit. Using this argument, it also has been postulated that excessive swirl should be a destabilizing factor when the recirculation vortex becomes so large that it entrains too much cold outside air. For such conditions there would be cool gas, rather than hot gas, that is forced upstream to mix with the partially premixed reactants.
3. A third reason that could explain why swirl is a stabilizing factor is that swirl can create *stagnation points* that act as bluff body flame holders. Either the stagnation point at the upstream end or at the downstream end of a recirculation vortex could be a point of flame attachment.
4. Another effect of swirl is that it can greatly increase the *rate of strain* imposed on a flame. That is, for fixed fuel and coaxial air flow rates, increasing the swirl velocity component can subject the reaction zone to velocity gradients (such as radial variations in the tangential velocity component) that convectively cool the flame and lead to strainout. Results below verify that excessive swirl causes flame blowout.

PREVIOUS ANALYSIS OF BLOWOUT LIMITS FOR NONSWIRLING FLAMES

In order to explain the measurements that are reported herein, it is necessary to cite two analyses that explain the blowout of nonswirling jet flames. The first approach was postulated by Vanquickenbourne and Van Tiggelen [15] and was extended by Kalghatgi [16, 17]. A flame is assumed to blow out when the local gas velocity near centerline (U_{CL}) exceeds the local turbulent burning velocity (S_T) of the flame base, which is assumed to be partially premixed. This simple concept is difficult to implement because the degree of local premixing is not known, the relation between the burning velocity and turbulence level in any premixed flame is in dispute, and it is a serious error to use mean concentration levels to infer the instantaneous concentration. That is, at a given location one may find very fuel-rich conditions at some times and fuel-lean conditions at other times such that the mean equivalence ratio is stoichiometric; a model could predict that such a location is ideal for flame stabilization when in fact no flame could exist there.

Kalghatgi's analysis [17] employed an empirical relation for burning velocity S_T given by Andrews et al. [18] such that at the flame liftoff position z:

$$U_{CL}(z) = S_T(z) = S_L\sqrt{\frac{u'l}{\nu}} \cdot \text{constant}, \tag{1}$$

where S_L is the maximum laminar burning velocity and ν is the kinematic viscosity. The quantity l is the mixing length in the jet; it is proportional to the liftoff height z. Kalghatgi then uses his own empirical observation that blowout occurs when the liftoff height z is 0.75 times the length of the attached flame, which is known to be proportional to the fuel tube inner diameter d_F [19]. Root-mean-squared velocity fluctuations u' are assumed to be proportional to U_{CL}, and U_{CL} can be shown to be $U_F(d_F/z)(\rho_F/\rho_A)^{1/2}$ since the jet is self-similar and the momentum flux, which is the integral of $\rho U^2(z)2\pi r\,dr$, is conserved. U_F is the fuel exit velocity. Kalghatgi substituted these quantities into Eq. 1 to yield a nondimensional relation for blowout velocity U_F:

$$\frac{U_F/d_F}{S_L^2/\alpha_F} = \text{Da}_K^{-1}, \tag{2}$$

where

$$\text{Da}_K^{-1} = 0.017\left(\frac{\alpha_F}{\nu_F}\right)\left(\frac{\rho_A}{\rho_F}\right)^{3/2}\left[\frac{4}{\theta_S}\left(\frac{\rho_F}{\rho_A}\right)^{1/2} - 5.8\right] \tag{3}$$

The right-hand side of Eq. 2 is interpreted by the present authors to be an inverse Damkohler number; Kalghatgi does not use such nomenclature. It depends only on fuel and air properties; typical

TABLE 1

Parameters Describing the Three Geometries and Three Fuels Used

System Configuration	A	B	C	D	E
Fuel	CH_4	CH_4	CH_4	0.67 CH_4 0.33 H_2 by volume	0.45 CH_4 0.55 H_2 by volume
d_A (cm)	3.14	2.22	1.44	1.44	1.44
d_F (cm)	0.48	0.34	0.22	0.22	0.22
d_F/d_A	0.15	0.15	0.15	0.15	0.15
$d_{F,0}/d_F$	1.42	1.41	1.44	1.44	1.44
Maximum heat release (kW)	70.0	75.5	15.5	33.4	62.0
S_L (cm/s) [27]	39	39	39	55	76
α_F (cm^2/s)	0.203	0.203	0.203	0.431	0.652
Da_K^{-1} (Kalghatgi, Eq. 5)	2.7	2.7	2.7	6.1	8.8
Da_B^{-1} (Broadwell, Eq. 5)	2.3	2.3	2.3	4.5	6.7
Da_0^{-1} measured $U_A = 0$	2.2	2.4	2.4	5.8	9.4

values are given in Table 1. Quantities ρ_F, α_F, and ν_F are the density, thermal diffusivity, and kinematic viscosity of the fuel. The quantity θ_S is the fuel mass fraction in a stoichiometric mixture. Kalghatgi showed that Eq. 2 is in good agreement with his measurements of U_F. Thus, for simple jet flames, the blowout velocity U_F is proportional to d_F and ${S_L}^2$.

A different approach was suggested by Broadwell, Dahm, and Mungal [20]; this analysis will be referred to as the BDM approach. Blowout is assumed to occur when the local fluid mechanical mixing rate, which is $U_{CL}(z)/\delta(z)$, exceeds the chemical reaction rate, which is proportional to ${S_L}^2/\alpha_S$. Such a concept is analogous to the criterion that was successfully used by Marble and Zukowski to explain the blowout of premixed flames stabilized by a rod [22]. $U_{CL}(z)$ is the centerline axial velocity, which varies as $U_F(d_F/z)(\rho_F/\rho_A)^{1/2}$, and δ is the jet halfwidth that is proportional to z. The liftoff position (z) at blowout in the BDM analysis is assumed to be proportional to the length of the attached flame, which is the distance required to mix fuel and air to their stoichiometric proportions and is shown to be proportional to the fuel tube inner diameter d_F. The BDM analysis leads to a blowout velocity U_F given by

$$\frac{U_F/d_F}{S_L^2/\alpha_F} = Da_B^{-1}, \tag{4}$$

where

$$Da_B^{-1} = \frac{(1+\Psi)^2}{4.8}\left(\frac{\rho_F}{\rho_A}\right)^{1/2}\frac{\alpha_F}{\alpha_S}, \tag{5}$$

Herein the quantity defined by Eq. 5 is interpreted to be an inverse Damkohler number although Broadwell et al. do not use such nomenclature. Ψ is the stoichiometric air-to-fuel mass ratio, α_S is the thermal diffusivity of the stoichiometric fuel–air mixture at the adiabatic flame temperature, and α_F is the thermal diffusivity of the fuel at the inlet temperature. Thus the final result of the BDM analysis is similar to that of Kalghatgi (Eq. 2). Both results agree with experiments even though the right-hand sides are functionally different. Typical values of the critical inverse Damkohler number Da_B^{-1} appear in Table 1.

In the present work, either Kalghatgi's approach or the BDM approach could be followed in plotting the results and assessing the effect of swirl. No definitive study has proven that one approach is superior. We have chosen the BDM approach and thus use Da_B^{-1}, given by Eq. 5, rather than Da_K^{-1}, given by Eq. 3, in plotting certain data because the BDM approach is the only one to successfully account for the presence of a coaxial air flow, which is used in the present experiment. Dahm and Mayman [21] and Dahm and Dibble [23] have extended the BDM concepts to correctly predict blowout curves for the case of a

simple jet surrounded by a coaxial air flow having a finite diameter, as well as for the somewhat different case of co-flowing air of infinite extent. In both cases the airflow dramatically changes the blowout limits; air velocity as low as 2% of the fuel velocity can cause blowout, and a new limit appears that is a minimum fuel velocity. The fact that Dahm's analysis can correctly predict these new physical trends as well as predict both the shape and magnitude of the blowout curves, for arbitrary exit geometry and using no new empirical constants, is very encouraging.

EXPERIMENTAL APPARATUS

A schematic of the swirl-stabilized flame apparatus is shown in Fig. 1. The swirl generator consists of four tangential air inlets that mix tangential air with axial air upstream of the burner. The swirling coaxial airflow surrounds a central fuel tube that injects fuel in the axial direction. Axial fuel injection is preferred because when the swirl is gradually reduced to zero, one recovers the important case of a jet flame with coaxial air that is documented in the literature; thus the swirl and no-swirl cases can be properly compared. Three different sized burners were used; their dimensions are given in Table 1. In all cases the ratio of the fuel tube inner diameter, denoted d_F, to the air tube diameter d_A at the throat was constant; the ratio of the fuel tube inner diameter to the outer diameter $d_F/d_{F,0}$ also was constant. Three different fuels were used: pure methane, a mixture of 0.67 methane and 0.33 hydrogen by volume, and a mixture of 0.45 methane and 0.55 hydrogen, as listed in Table 1. Flow rates were metered to an accuracy of 5.5% using a system of 15 calibrated choked orifices and 4 rotameters. A small correction to fuel velocity was made for compressibility effects for about 10% of the data collected. That is, for most cases fuel velocity U_F is determined by dividing measured fuel mass flow by the fuel tube area and by the standard density of the fuel gas. For 10% of the data, the exit Mach number of the fuel was in the range 0.3–0.6 so the exit density of the fuel that was used was determined from standard compressible flow tables and the known stagnation pressure and temperature.

To obtain a strong recirculation vortex, a diverging metal quarl section is placed downstream of the cylindrical throat. Upstream of the tangential air inlets, the axial air profile was made uniform by using flow straighteners and a 30-mesh screen. Additional experimental details are given in Ref. 1.

The swirl number S in this study is identical to the conventional definition given by Ref. 6, i.e., S is the ratio of the flux of angular momentum passing through the throat to the flux of axial momentum, divided by the throat radius. Thus

$$S = \int_{d_{F,0}/2}^{d_A/2} (\rho r u_\theta u_z) 2\pi r \, dr \Big/ \left[\int_{d_{F,0}/2}^{d_A/2} \rho (u_z^2 - u_\theta^2/2) 2\pi r \, dr \cdot (d_A/2) \right]. \quad (6)$$

Use of Eq. 6 eliminates any need to measure static pressure [24]. Laser velocimetry was used to measure profiles of u_θ and u_z within the Vycor glass throat, and thus the swirl number S was deduced using Eq. 6. It was found that a convenient way to monitor S was to monitor the mass flow rates of the axial air (m_A) and tangential air (m_θ) to first determine a geometric swirl number (S_g), which is defined as [25]

$$S_g = \frac{\pi r_0 d_A}{2A_t} \left(\frac{m_\theta}{m_\theta + m_A} \right)^2. \quad (7)$$

A_t is the total area of the four tangential air inlets and r_0 is the radius of the air tube where the tangential air is injected. S was measured using laser velocimetry for 17 different conditions and in all cases S was found to be $0.25S_g$ to within a standard deviation of $\pm 6\%$. Using this calibration, it was possible to deduce S directly from the mass flow measurements.

TYPES OF FLAMES OBSERVED

Just prior to flame blowout, three distinct types of flames were observed, as shown in Fig. 1: (1) lifted flames, which look like lifted simple jet flames; (2) type 1 jet-like flames, which look like long, attached jet flames but blow out suddenly

without lifting off; and (3) short, type 2 flames, which also blow out suddenly without rising (i.e., without appreciable liftoff).

The lifted flame (Fig. 1a) is blue near the base, indicating appreciable fuel–air mixing in the liftoff region. The liftoff height of these swirl flames differs from that of a simple jet flame. For the swirl flames, the liftoff height is constant and independent of fuel velocity; the flame appears to stabilize just downstream of the recirculation zone. For a simple jet flame, liftoff height increases with fuel jet velocity. The second type of blowout occurs for type 1 jet-like flames (Fig. 1b). These long flames blow out without appreciable liftoff, indicating that the upstream portion of the recirculation zone is stabilizing the flame. When the fuel velocity exceeds a critical value, the conditions in the downstream region of the recirculation zone are not favorable for flame stabilization so the entire jet flame suddenly blows out. The third type of flame is the short, type 2 flame, which always appears to be blue. This type of flame has a strong recirculation zone and blowout occurs when the fuel velocity is reduced significantly. The short type 2 flames do not blow out due to excessive fuel velocity, but because the lean flame is strained out by the strong recirculation vortex.

RESULTS: EFFECTS OF SWIRL, COAXIAL AIR

The blowout limits for the intermediate size burner and methane fuel are shown in Fig. 2. U_F represents fuel velocity at the exit of the fuel tube when blowout occurs. U_A represents the axial component of the air velocity at the throat location defined in Fig. 1, and is determined from mass flow measurement. The first observation is that the blowout limits are defined by peninsula-shaped curves, each corresponding to a different swirl number. Two questions arise that are discussed below: how does existing theory explain the observed shape of the curves, and why does the size of the peninsula-shaped stable region increase as swirl is increased? It is first noted that all of the blowout curves in Fig. 2 intercept the y axis at $U_F = 61.7$ m/s; this point corresponds

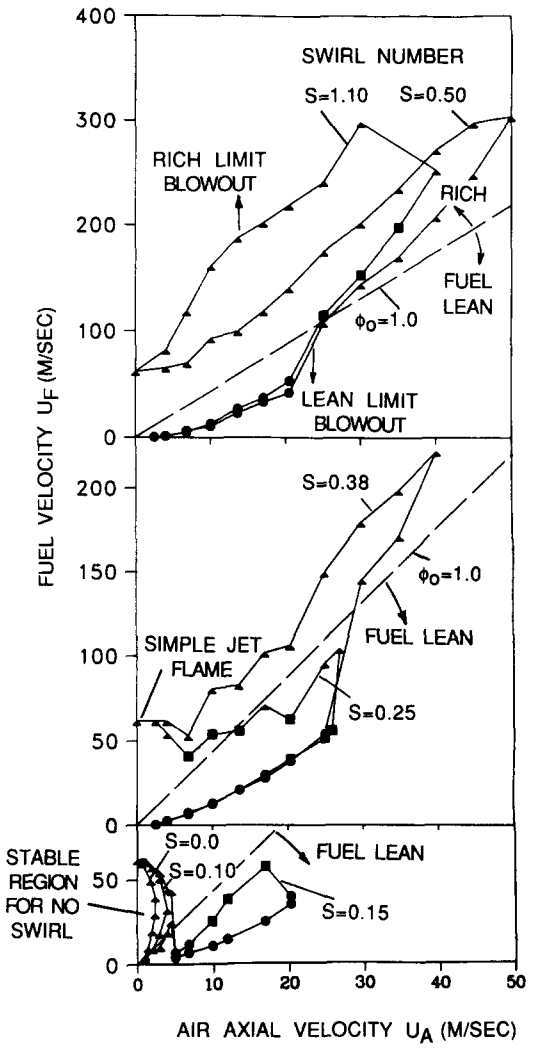

Fig. 2. Increase in the flame stability region due to swirl. Intermediate-sized burner and methane fuel. $d_A = 2.22$ cm, $d_F = 0.34$ cm; flame shape at blowout: ▲, lifted; ■, long, jet-like, no liftoff; ●, short, recirculating, no liftoff.

to the case of a simple jet flame with no coaxial air. This y-axis intercept (Fig. 2), as well as the corresponding y-axis intercepts measured for the different burner sizes, are in reasonable agreement with the results of Kalghatgi's findings for nonswirling jet flames, as shown in Table 1.

The fact that the stable region in Fig. 2 is peninsula shaped indicates that blowout can be caused by either increasing fuel velocity above a "rich

limit" or by reducing U_F below a "lean limit." The ratio of these two limits is the turndown ratio, which should be maximized for practical combustors. Figure 2 shows that the turndown ratio can be increased by increasing the swirl. It is expected that the lean limit in Fig. 2 should pass through the origin; if it intercepted the x axis, infinitely lean flames would be possible. It is noted that each curve in Fig. 2 extends to the right to only a certain extent; there is a maximum air velocity U_A above which no stable flame is possible. This implies that for a given air velocity, there is a minimum swirl number limit. For example, for $U_A = 28$ m/s in Fig. 2, the minimum swirl number is 0.25. Operation at swirl number below 0.25 produces a peninsula-shaped region that does not extend sufficiently far to the right in Fig. 2 to overlap the vertical line $U_A = 28$ m/s.

One of the curves in Fig. 2, namely the zero-swirl curve, can be predicted accurately by the existing theory of Dahm and Mayman [21]. Dahm, and to a limited extent Vranos [26] and Yuasa [11], also have measured zero-swirl blowout curves similar to the one in Fig. 2. It is concluded from the zero-swirl curve of Fig. 2 that coaxial air alone (with no swirl) has a destabilizing effect on a flame. That is, the maximum fuel velocity in Fig. 2 is reduced from 61.7 m/s for zero coaxial air to 40 m/s for air velocity of 2.4 m/s. For air velocity above 2.4 m/s, the flame is not stable for any fuel velocity. It also can be concluded from Fig. 2 that even small amounts of swirl have a stabilizing effect; the semicircular stable region for $S = 0.1$ is larger than the stable region for zero swirl. However, the low-swirl, nonrecirculating flames are still less stable than the pure diffusion flame (i.e., the y-axis intercept in Fig. 2) because the stabilizing effects of swirl do not yet exceed the destabilizing effects of coaxial air.

On the other hand, a sufficient amount of swirl has a strong stabilizing effect on the flame. Figure 2 quantifies this effect in an unambiguous manner. It is seen that the fuel velocity can be increased by a factor of 5 over that of a simple jet flame (from 61.7 to 298 m/s). This is a significant improvement and allows the burner to provide five times the heating power (in kilowatts) of a nonswirling flame having the same fuel tube diameter. Although the stabilizing effects of swirl are well known, quantitative comparisons of swirl burners to non-swirling jet flames, such as Fig. 2, are few. Yuasa [11] reports a fourfold improvement in the maximum fuel velocity due to swirl.

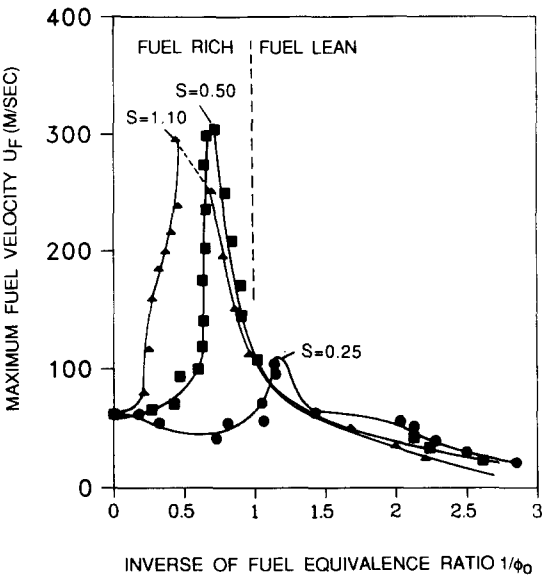

Fig. 3. Optimum overall fuel equivalence ratio required to maximize fuel velocity.

Figure 3 shows another way to plot the flame blowout limits that can be more useful for practical design. In practical cases the overall fuel equivalence ratio may be specified. Figure 3 shows that there is an equivalence ratio that provides optimum fuel velocity and heat release for a given swirl number. For overall rich conditions at the burner exit (i.e., when outside entrained air is available) such as $1/\phi = 0.5$, it is seen that maximum fuel flow rate can be achieved by operating at the highest swirl number of 1.1. For fuel-lean conditions such as $1/\phi = 2.0$, lower swirl is seen to be somewhat preferable. Thus rich flames are more stable if high swirl is provided while lean flames are limited to smaller amounts of swirl, which is in agreement with observations of Leuckel [9]. It is believed that rich flames benefit from the increased mixing of air into the flame caused by the swirl-induced vortex, while lean flames extinguish when all the excess air is rapidly mixed with the fuel.

EFFECT OF BURNER SIZE, FUEL TYPE

The effect of burner size on flame blowout can be observed by comparing Figs. 2, 4, and 5. Three geometrically similar burners were operated using methane. Fuel tube diameters were 0.22, 0.34, and 0.48 cm as given in Table 1. For zero coaxial air, the blowout velocities of the simple jet flames are observed to increase from 39.4 m/s (Fig. 4) to 61.7 m/s (Fig. 2) to 80.5 m/s (Fig. 5) as fuel tube diameter increases. Thus, the absolute values of U_F at blowout for no swirl or coaxial air are in good agreement with Kalghatgi's previous data, as represented by Eq. 2, as well as with the BDM analysis, as represented by Eq. 4. As coaxial air and swirl is added, the general shapes of

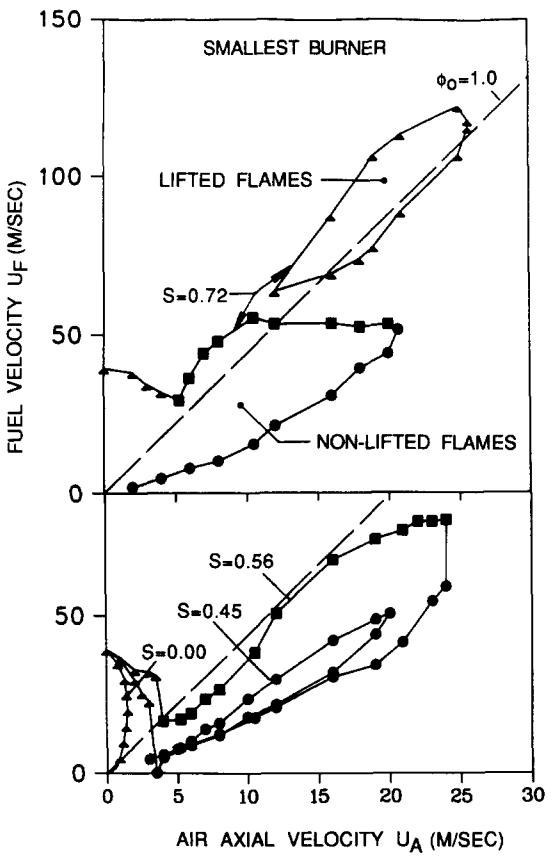

Fig. 4. Effect of burner size on blowout limits; smallest burner, methane fuel. Note that smallest burner has lower fuel velocity at blowout than intermediate size burner (Fig. 2). Symbols same as Fig. 2; $d_A = 1.44$ cm, $d_F = 0.22$ cm.

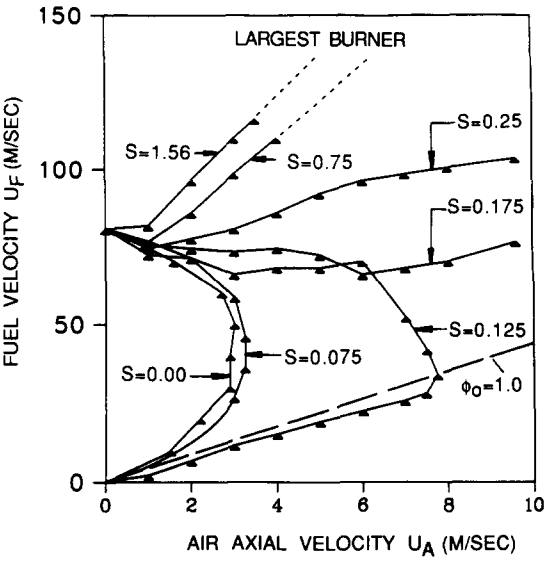

Fig. 5. Effect of burner size on blowout limits; largest burner, methane fuel. Symbols same as Fig. 2; $d_A = 3.14$ cm, $d_F = 0.48$ cm. Note: curves for $S = 0.175$, 0.25, 0.75, and 1.56 are terminated because of fuel or air flow metering limitations.

the curves in Figs. 4 and 5 are similar to those in Fig. 2. It is noted that for the conditions of Fig. 4, i.e., using the smallest burner, the stable region is no longer peninsula-shaped but a disjoined stable region occurs. These lifted flames only can be created by first increasing the velocity of the fuel jet such that it penetrates the recirculation zone, and then igniting the flame. Unlike a jet flame, these particular lifted flames cannot be achieved by starting with an attached flame and then increasing fuel velocity. In Fig. 5, only portions of the blowout curves for S greater than 0.125 were measured due to limitations in metering the fuel and air.

The effect of adding hydrogen to the methane fuel is shown by comparing Figs. 6 and 7 to Fig. 4. The burner size is the same for Figs. 4, 6, and 7 but the amount of hydrogen in the fuel is 0%, 33%, and 55% by volume, respectively. In all cases, the methane–hydrogen mixture was premixed in a high-pressure tank and all measurements were made with the same tank of fuel to ensure repeatability of fuel composition. The blowout velocity for zero swirl and zero coaxial air increases from 39.4 m/s (Fig. 4) to 90.2 m/s (Fig. 6) to 182.8

m/s (Fig. 7) as hydrogen is added. These blowout velocities for nonswirling H_2–methane jet flames agree with Kalghatgi's correlation (Eq. 2); values of the maximum laminar burning velocity S_L for the methane-hydrogen mixtures were taken from Ref. 27, other mixture properties were determined from Ref. 28.

It is noted that if it is desired to operate the present flame in an overall fuel-lean condition, some swirl is required. All of the zero swirl stable regions reported in Figs. 2, 4, 5, 6, and 7 lie above the line marked $\phi_0 = 1.0$, where overall fuel-rich conditions occur. The only stable lean flames (i.e., below the $\phi_0 = 1$ line) are those with swirl.

COMPARISON OF ZERO-SWIRL BLOWOUT CURVES WITH PREDICTIONS OF THE DAHM-MAYMAN ANALYSIS

In each of Figures 2, 4, 5, 6, and 7, one of the flame blowout curves corresponds to zero swirl. It is useful to compare these curves to the predictions of the Dahm and Mayman (D-M) analysis [21] because the experimental data of the present study represents a range of new conditions, including methane-hydrogen mixtures and various air velocities and air tube diameters, that extend the range of the previous comparisons. The D-M analysis adds a coaxial airflow to the BDM analysis of a simple jet flame, which was described by Eqs. 4 and 5. The D-M analysis assumes that the actual geometry, which is a central fuel jet surrounded by a coaxial air flow, is identical in the far field to a hypothetical single jet of premixed fuel and air, for which the flame blowout limits are given by Eqs. 4 and 5. The analysis introduces no new empirical parameters. The only parameter is the constant 4.8 in Eq. 5, which has been shown to be universal for all jet flames, with and without coaxial air. The predicted shape of the flame blowout curve for zero swirl is given by [21]

$$U_A{}^2 = (\alpha\beta^{4/3}\eta d_A{}^{2/3})U_F{}^{4/3} - (\beta\eta)U_F{}^2. \qquad (8)$$

The parameter α is $[(S_L{}^2/\alpha_S)(1 + \mathrm{AF})^2/4.8]^{2/3}$, where AF is the stoichiometric air–fuel mass ratio, which is 17.2 for methane. The parameter β is $(\rho_F/\rho_A)(d_F/d_A)^2$ and η is $1/[1 - (d_{F,0}/d_A)^2]$; parameters $d_{F,0}$, etc. were defined previously and appear in the Nomenclature and in Table 1. For methane–air flames, α is 808 $(\mathrm{s})^{-2/3}$ and for all

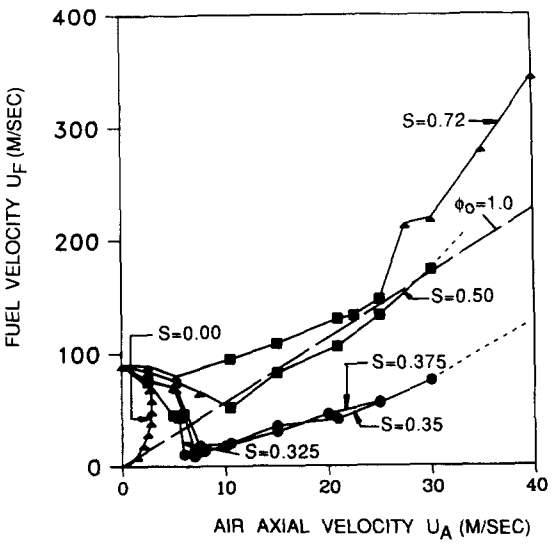

Fig. 6. Effects of 33% hydrogen enrichment of methane fuel on blowout limits of smallest burner. (d_A = 1.44 cm, d_F = 0.22 cm; symbols same as in Fig. 2). Only portions of rich limits shown.

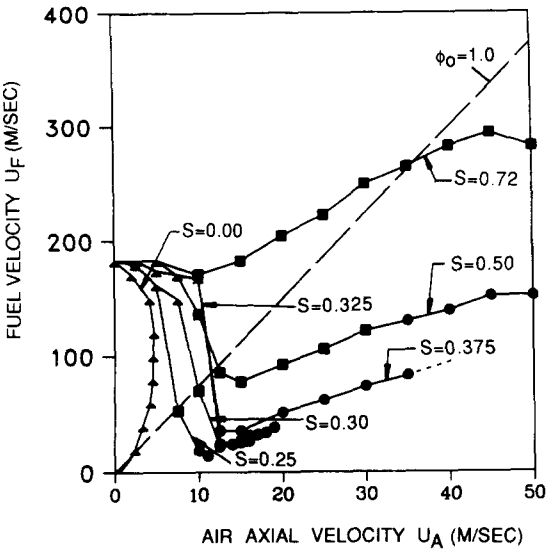

Fig. 7. Effect of 55% hydrogen enrichment of methane fuel on blowout limits of smallest burner (symbols same as Fig. 2). Only rich limits shown.

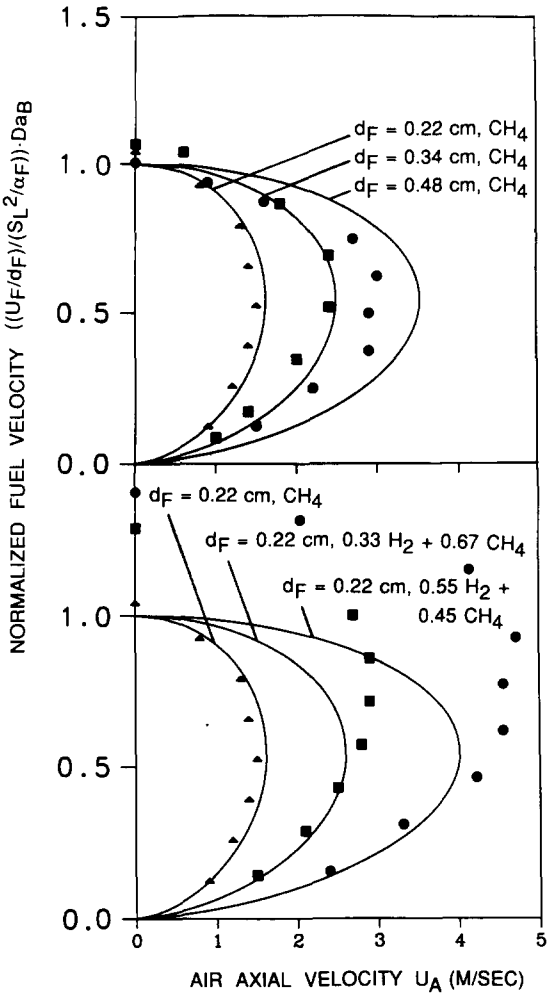

Fig. 8. Comparison of zero-swirl blowout data to analysis of Dahm and Mayman. Predictions: solid lines, computed using Eq. 8; Da_B, critical Damkohler number, Eq. 5, values in Table 1. For all curves $d_F/d_A = 0.15$.

burner geometries in the present study β is 0.0124 and η is 1.05.

A comparison of the present results to the predicted blowout curves for zero swirl is shown in Fig. 8. It is seen that for the case of methane fuel in the top portion of Fig. 8, the D-M analysis predicts flame blowout curves that are in reasonably good agreement with the present measurements for zero swirl. Most importantly, the physics of the analysis appears to be correct because it properly predicts that blowout occurs by either sufficiently increasing or sufficiently decreasing the fuel velocity for a given air velocity. For the two cases of hydrogen-enriched fuel shown in Fig. 8, the effect of air velocity is properly predicted but the vertical extent of the predicted curves does not agree with the data. The reason for the disagreement is believed to be due to the large uncertainty in the maximum laminar burning velocity of methane–hydrogen mixtures. Values of S_L used in Fig. 8 were taken from Ref. 27 and are given in Table 1. Although there is a 40% difference between the measured y-axis intercept in Fig. 8 and theory, the data are scaled by $S_L{}^2$ so if the true value of S_L is actually 18% larger than the empirical values used, all the curves in Fig. 8 would pass through a y-axis intercept of unity and would agree with theory. The disagreement could instead be due to weakness in the BDM analysis, but this is less likely since the BDM analysis accurately predicts the blowout of pure methane flames (see Fig. 8, top curves) and pure hydrogen flames [20].

ANALYSIS: CORRELATION OF RICH BLOWOUT LIMITS WITH SWIRL VELOCITY

Previous analyses of nonswirling flames have shown that blowout can be explained as the condition that occurs when a local inverse Damkohler number $(U_{CL}/\delta)(S_L{}^2/\alpha)$ exceeds some critical value, which leads to Eq. 4. Because U_{CL} and δ are local conditions at the location where the lifted flame blows out, it is necessary to relate U_{CL} and δ to the throat conditions U_F, d_F, S, etc.

It is proposed that one can represent lifted and jet-like swirl flames (Figs. 1a and b) as a fuel jet that has penetrated through a toroidal vortex, as shown in Fig. 9. The effect of swirl therefore is to reduce the local centerline velocity U_{CL}, at every axial location, below that of the nonswirling case (U_j), and this should have a stabilizing effect on a flame. Thus

$$U_{CL}(z) = U_j(z) - U_v(z), \tag{9}$$

where subscript j denotes conditions within a nonswirling jet and U_v is the magnitude of the velocity induced by the recirculation vortex at the down-

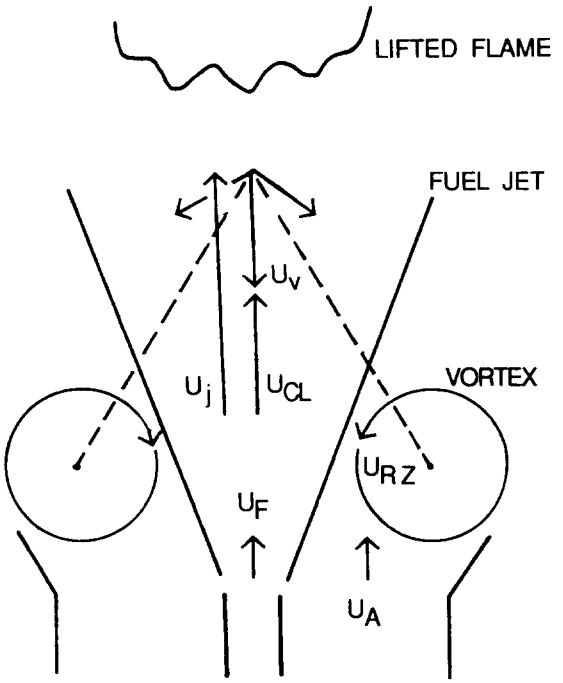

Fig. 9. Schematic showing how swirl stabilizes a flame. Note: vortex-induced velocity (U_v) reduces the actual centerline velocity (U_{CL}) below that of a nonswirling jet (U_j).

stream location where the lifted flame blows out. The velocity induced at a distance z from a free vortex is the vortex circulation divided by $2\pi z$; similarly the experimental data of Ref. 1 show that U_v is proportional to the vortex circulation, which is proportional to the characteristic recirculation zone velocity (U_{RZ}) multiplied by the recirculation zone radius (b). U_{RZ} is defined [1] as the volumetric flow rate of gas that recirculates divided by the maximum recirculation zone radius squared times pi. Measured values of U_{RZ} are reported in Ref. 1, which shows that U_{RZ} is, in turn, proportional to the characteristic angular velocity of air at the throat (U_θ), which is defined as the product of $U_A \cdot S$; thus

$$U_v \sim \frac{U_{RZ} b}{2\pi z}, \quad U_{RZ} \sim U_\theta - U_{\theta,c}, \quad U_\theta \equiv U_A \cdot S. \tag{10a}$$

$U_{\theta,c}$ is the critical value of angular velocity required to create a recirculation zone. The recirculation zone radius (b) is proportional to $d_A(1)$.

The centerline velocity induced by a jet (U_j) that appears in Eq. 9 is known to be $U_F(d_F/z)(\rho_F/\rho_A)^{1/2}$ because the total momentum flux of jet fluid is conserved. Furthermore, the characteristic radial extent of a jet δ is proportional to z. The axial location z where blowout occurs is found to be proportional to flame length, L, based on theoretical and experimental results presented in Refs. 16 and 20. The flame length L is the location where fuel and air have mixed to stoichiometric proportions and is given by $d_F(\rho_F/\rho_A)^{1/2}(1+\psi)$, where ψ is the stoichiometric air–fuel ratio [20].

Therefore, if one used the BDM concept that was used to derive Eq. 5, blowout should occur where

$$(U_{CL}/\delta)/(S_L{}^2/\alpha_S) = 1/\epsilon, \tag{10b}$$

where ϵ is a universal constant that is 4.8 [20]. By substituting Eqs. 9 and 10a into Eq. 10b, and using the relations for U_j, δ, z, and L described in the previous paragraph it follows that the effects of swirl can be represented by the following relation:

$$\frac{U_F/d_F}{S_L{}^2/\alpha_F} \cdot \mathrm{Da}_B = 1 + \frac{(U_A S - U_{\theta,c})/d_A}{S_L{}^2/\alpha_F} \cdot \mathrm{Da}_B \cdot c_1 (d_A/d_F)^2, \tag{11}$$

where Da_B is given by Eq. 5 and c_1 is a constant. Equation 11 indicates that the maximum fuel velocity U_F should scale linearly with U_A and the slope of the U_F vs. U_A line should be proportional to swirl number S. Equation 11 illustrates the physical reason why swirl helps to stabilize the flame; there is a competition between the fuel jet and the recirculation vortex. Increasing the jet velocity U_F increases U_{CL}, which is destabilizing, and increasing the vortex velocity U_{RZ} by increasing swirl number S or U_A reduces U_{CL}, which is stabilizing.

To test the scaling that lead to Eq. 11, the rich blowout limits alone are plotted in Figs. 10 and 11 for two burner sizes. It is seen that U_F does scale linearly with U_A and that the slope of the U_F vs. U_A curve is proportional to swirl number, as is predicted by the analysis. This suggests that the proposed mechanism for the stabilizing effect of

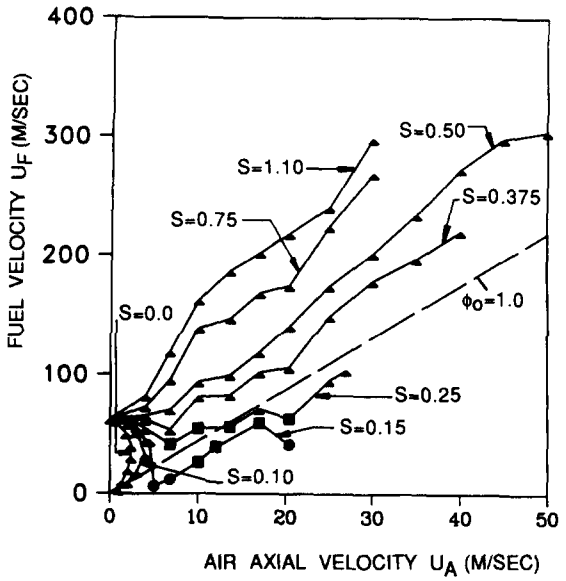

Fig. 10. Maximum fuel velocity limit for intermediate size burner using methane. Symbols same as Fig. 2.

swirl, i.e., the reduced centerline axial velocity, is correct.

Another conclusion that results from Eq. 11 is that swirl number S is not a fundamental governing parameter. Instead it is the product of U_A and S

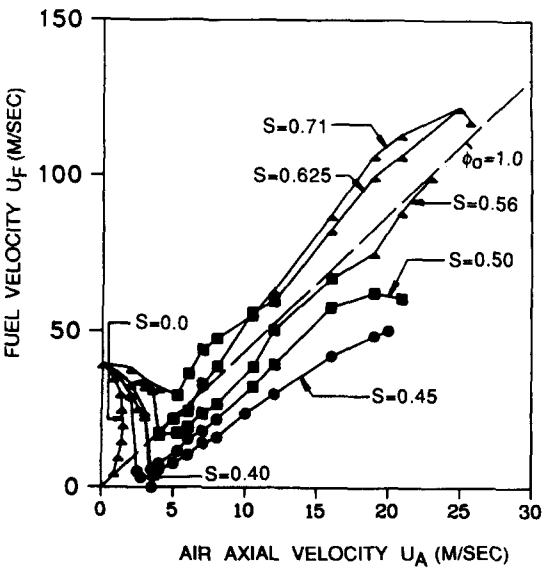

Fig. 11. Maximum fuel velocity at blowout for smallest burner using methane. Symbols same as Fig. 2.

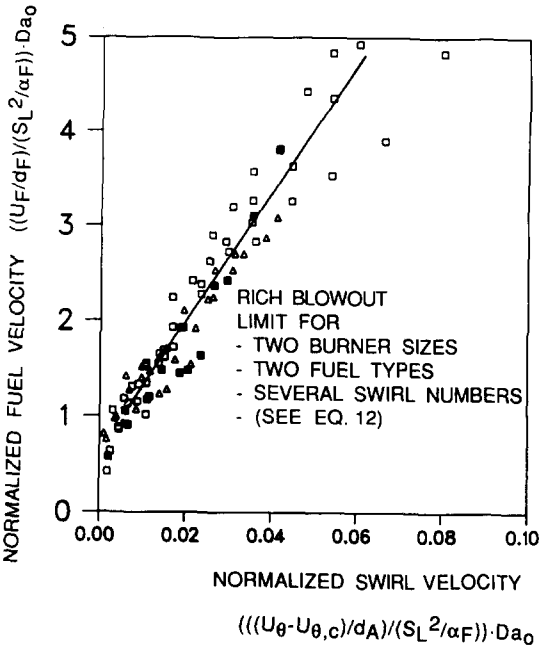

Fig. 12. Collapse of rich limit blowout curves of Figs. 6, 10, and 11 for different burner sizes and fuels to a general curves using the Damkohler number parameter suggested by Eq. 12. △, Methane, smallest burner, $U_{\theta,c} = 5.0$ m/s; □, Methane, intermediate burner, $U_{\theta,c} = 0.75$ m/s; ■, 0.67 CH_4, 0.33 H_2, smallest burner, $U_{\theta,c} = 4.0$ m/s. Values of Da_0 given in Table 1.

which appears in Eq. 11. Because the product of U_A and S is defined as the characteristic angular velocity at the throat U_θ, Eq. 11 can be written as

$$\frac{U_F/d_F}{S_L^2/\alpha_F}\cdot \mathrm{Da}_B = 1 + \frac{(U_\theta - U_{\theta,c})/d_A}{S_L^2/\alpha_F} \cdot \mathrm{Da}_B \cdot c_1 (d_A/d_F)^2, \qquad (12)$$

which identifies the inverse Damkohler number based on U_θ as the general governing parameter. To test the generality of Eq. 12, the rich blowout limit data are replotted in Fig. 12 using the parameters suggested by Eq. 12; it is seen that the data collapse to form a single linear curve. The value of c_1 that is obtained from Fig. 11 is 1.50; this constant is believed to be geometry dependent. However, the linear correlation seen in Fig. 12 is a general result because the data plotted represent a wide range of different values of U_θ, d_F, d_A, and S_L.

CONCLUSIONS

1. A coaxial air flow with no swirl has a destabilizing effect on a nonpremixed jet flame; adding a small amount of swirl to the airflow slightly improves stability, but the maximum fuel flow rate achievable is still less than the case of no coaxial air. However, if sufficient swirl velocity is imparted to create a recirculation zone, up to a fivefold improvement in flame stability is measured.
2. At the rich blowout limit, the effect of swirl is to create a vortex which reduces the centerline fuel jet velocity. This concept explains the observed trends in the data and suggests that the two governing parameters are Damkohler numbers based on fuel jet and swirling air flow properties, as given by Eq. 12.
3. Using the proper nondimensional parameters, the measured blowout curves obtained for a range of swirl numbers, air and fuel velocities, burner sizes and fuel types were found to collapse to a single general curve.
4. For the geometry considered, if overall lean conditions are desired, some amount of swirl is required to achieve a stable flame. However, excessive swirl also can destabilize a lean flame, so an optimum amount of swirl exists.

The research reported herein is supported by the Gas Research Institute under contract 5087-260-1443. The contract monitor is J. Kezerle. The authors wish to acknowledge useful discussions with Professor W. J. A. Dahm concerning his analysis.

REFERENCES

1. Tangirala, V., and Driscoll, J. F., *Combust. Sci. Technol.* 60(1-3):143 (1988).
2. Tangirala, V., Chen, R. H., and Driscoll, J. F., *Combust. Sci. Technol.* 51:75 (1987).
3. Chen, R. H., and Driscoll, J. F., *Twenty-Second Symposium (International) on Combustion*, The Combustion Institute, Pittsburgh, 1988, p. 531.
4. Chen, R. H., Driscoll, J. F., Kelly, J., and Namazian, M., Combust. Sci. Technol., 1990 (in press).
5. Syred, N., and Beer, J. M., *Combust. Flame* 23:143 (1974).
6. Beer, J. M., and Chigier, N., *Combustion Aerodynamics*, Applied Science Publishers, London, 1972.
7. Buckley, P. L., Craig, R. R., Davis, D. L., and Schwartzkopf, K. G., *AIAA J.* 21:733-740 (1983).
8. Samimy, M., and Langenfeld, C. A., *AIAA J.* 26, 12, p. 1442 (1988).
9. Leuckel, W., and Fricker, N., *J. Inst. Fuel* 49:152 (1976).
10. Rawe, R., and Kremer, H., *Eighteenth Symposium (International) on Combustion*, The Combustion Institute, Pittsburgh, 1981, p. 667.
11. Yuasa, S., *Combust. Flame* 66:181 (1986).
12. Milosavljevic, V., Taylor, A. M. K. P., and Whitelaw, J. H., *Combust. Flame* (in press).
13. Godoy, F., and Lockwood, F. C., *Combust. Sci. Technol.* 44, 319 (1987).
14. Hillemanns, R., Lenze, B., and Leuckel, W., *Twenty-First Symposium (International) on Combustion*, The Combustion Institute, Pittsburgh, 1986, p. 1445.
15. Vanquickenbourne, L., and Van Tiggelen, A., *Combust. Flame* 10:59 (1966).
16. Kalghatgi, G., *Combust. Sci. Technol.* 26:233 (1981).
17. Kalghatgi, G., *Combust. Sci. Technol.* 41:17 (1984).
18. Andrews, G. E., Bradley, D., and Lwakabamba, S. B., *Combust. Flame* 24:285-304 (1975).
19. Hawthorne, W. R., Weddell, D. S., and Hottel, H. C., *Third Symposium (International) on Combustion*, The Combustion Institute, Pittsburgh, 1943, p. 266.
20. Broadwell, J. E., Dahm, W. J. A., and Mungal, M. G., *Twentieth Symposium (International) on Combustion*, The Combustion Institute, Pittsburgh, 1985, pp. 303.
21. Dahm, W. J. A., and Mayman, A. G., University of Michigan Report GRI 5087-260-1443-2; *AIAA J.* June, 1990 (in press).
22. Lewis, B., and Von Elbe, G., *Combustion Flames and Explosions of Gases*, 2nd ed., p. 440, Academic, New York, 1961, p. 440.
23. Dahm, W. J. A., and Dibble, R. W., *Twenty-Second Symposium (International) on Combustion*, The Combustion Institute, Pittsburgh, 1989, p. 801.
24. Ribiero, M. M., and Whitelaw, J. H., *J. Fluid Mech.* 96:769 (1980).
25. Claypole, T. C., and Syred, N., *Eighteenth Symposium (International) on Combustion*, The Combustion Institute, Pittsburgh, 1981, p. 81.
26. Vranos, A., Taback, E. D., and Shipman, C. W., *Combust. Flame* 12:253-260 (1968).
27. Yu, G., Law, C. K., and Wu, C. K., *Combust. Flame* 63:339-347 (1986).
28. *Technical Data Book—Petroleum Refining*, 3rd ed., American Petroleum Institute, 1976.

Received 11 April 1989; revised 23 June 1989